Preparation and Thermal Properties of Multiwalled Carbon Nanotube/Polybenzoxazine Nanocomposites

Jieh-Ming Huang,[1] Ming-Feng Tsai,[1] Shung-Jim Yang,[1] Wei-Ming Chiu[2]

[1]*Department of Chemical and Materials Engineering, Vanung University, 1, Van Nung Road, Chung-Li 32054, Taiwan*
[2]*Department of Chemical and Materials Engineering, National Chin-Yi University of Technology, Taiping City, Taichung County 411, Taiwan*

Received 9 July 2009; accepted 3 February 2011
DOI 10.1002/app.34290
Published online 10 June 2011 in Wiley Online Library (wileyonlinelibrary.com).

ABSTRACT: In this study, we prepared nanocomposites comprising multiwalled carbon nanotubes (MWCNTs) and polybenzoxazine (PBZ). The MWCNTs were purified through microwave digestion to remove most of the amorphous carbon and metal impurities. After purification, MWCNTs were treated with H_2SO_4/HNO_3 (3 : 1) to introduce hydroxyl and carboxyl groups onto their surfaces. Raman spectroscopy revealed the percentage of nanotube content improved after prolonged microwave treatment, as evidenced by the decrease in the ratio of the D (1328 cm^{-1}) and G (1583 cm^{-1}) bands. For the untreated MWCNTs, the I_D/I_G ratio was 0.56. After microwave treatment for 40 min, the value decreased to 0.29, indicating that the percentage of nanotube content improved. Dynamic mechanical analyses (DMAs) revealed that the storage moduli and the T_gs of the MWCNTs/PBZ nanocomposites were higher than that of the pristine PBZ. This is due to the nanometer-scale MWCNTs restricting the motion of the macromolecular chains in the nanocomposites. Transmission electron microscopy (TEM) image revealed that the MWCNTs were well dispersed within the PBZ matrix on the nanoscale when the MWCNT content was less than 2.0 phr. The coefficient of thermal expansion (CTE) of the nanocomposites decreased on increasing the MWCNTs content. © 2011 Wiley Periodicals, Inc. J Appl Polym Sci 122: 1898–1904, 2011

Key words: carbon nanotubes; nanocomposites; thermal properties; Raman spectroscopy

INTRODUCTION

Polybenzoxazines (PBZs) are a new class of thermosetting polymers that possess some physical properties similar to those found in traditional phenolic resins, such as high heat resistance and good flame retardance,[1] and others physical properties, such as high glass transition temperatures, large moduli, low water absorption, low dielectric constant, and near-zero shrinkage on curing, that improve on the limitations of conventional phenolics and epoxy resins.[2–4] In addition, PBZs can be polymerized via a thermally induced ring-opening polymerization without the use of a strong acid or base as a catalyst, and thus, no toxic gases or other byproducts are generated during polymerization. The molecular structures of PBZs offer enormous design flexibility, allowing the properties of the cured materials to be tailored for a wide range of applications.

Multiwalled carbon nanotubes (MWCNTs) have been attracting considerable attention not only because of their unique physical properties but also because of their potential applications in various fields.[5–7] MWCNTs exhibit an exceptionally high aspect ratio in combination with low density, as well as high strength and stiffness, which make them a potential candidate for the reinforcement of polymeric materials.[8,9] However, the presence of various impurities including amorphous carbon and other metal catalyst particles makes it difficult to disperse MWCNTs in any solvent or polymer matrices. These impurities are responsible for the poor properties of carbon nanotube (CNT) reinforced composites.[10] Despite many advantageous properties of MWCNTs/polymer composites, the studies of MWCNTs/PBZ nanocomposites are still limited. Recently, Yang et al.[11] investigated the effects of MWCNTs on the curing behavior and properties of the benzoxazine-epoxy-phenolic (BEP) ternary system. They found that the addition of MWCNTs decreased the coefficient of thermal expansion (CTE) of the composites. Chen et al.[12] reported that the surface carboxyl groups catalyzed the ring-opening reaction of benzoxazine and thus decreased the curing temperature of the system. Cui et al.[13] suggested that two factors affect the performance of MWCNTs formed nanocomposites: the degree of dispersion of the MWCNTs in

Correspondence to: J.M. Huang (jiehming@mail.vnu.edu.tw).

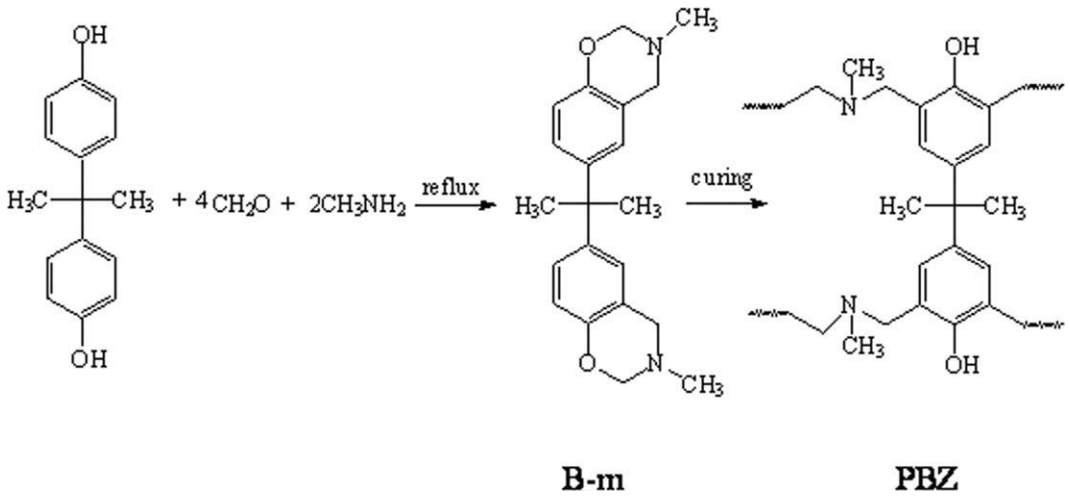

Scheme 1 Preparation of benzoxazine monomer and polybenzoxazine.

the matrix and the degree of interfacial adhesion between the MWCNTs and host matrix. In addition, it has been reported that the mechanical property of PBZ can be reinforced by the addition of carbon fiber.[14] Jang et al. investigated the effects of surface treatments on the mechanical properties of carbon fiber/PBZ composites. They found that both oxygen plasma treatment and nitric acid treatment were efficient in the enhancements of the interlaminar shear strength and flexural strength of carbon fiber/PBZ composites. Despite many studies on MWCNTs reinforced composites, the study of microwave-purified MWCNTs/PBZ nanocomposites has not been reported.

In this study, we combined microwave digestion and acid treatments to purify and functionalize MWCNTs. Then, we blended modified MWCNTs with benzoxazine monomer to prepare MWCNTs/PBZ nanocomposites. Herein, we evaluate the purity of the samples by Raman spectroscopy. We also discuss their morphology and thermal mechanical properties of the nanocomposites using scanning electron microscopy (SEM), transmission electron microscopy (TEM), and dynamic mechanical analysis (DMA).

EXPERIMENTAL

Materials

Bisphenol-A, formaldehyde, and methylamine were purchased from Aldrich Chemical Co. (Milwaukee, WI, USA) and used without further purification. Benzoxazine (B-m type) was synthesized from bisphenol-A, formaldehyde, and methylamine, according to the procedure presented in Scheme 1.[1,15] MWCNTs were purchased from Conyuan Biochemical Technology (Taiwan). These MWCNTs, which had been produced via chemical vapor deposition (CVD), had lengths of up to a few micrometers and diameters between 20 and 50 nm.

Purification and modification of MWCNTs

In this system, we used microwave to eliminate the metal catalysts and amorphous carbon. In a typical purification experiment, MWCNTs (0.5 g) were placed in a 250-mL Pyrex vessel and dispersed in 3*M* HNO_3 (100 mL) under ultrasonic vibration for 30 min. The samples were then placed in a microwave-accelerated reaction system operated at 300 W and 120°C for 40 min. After microwave digestion, the suspensions were filtered through 0.45-μm Teflon membranes, and the remaining solids were washed with deionized water until the pH reached ~ 7. The samples were then dried in an oven at 100°C for 8 h. Modification of the MWCNTs was performed by mixing a sample of the microwave-purified MWCNTs (0.5 g) with concentrated H_2SO_4 (98%, 30 mL) and HNO_3 (65%, 10 mL). The resulting mixture was then magnetically stirred for 4 h at 80°C. The solid was filtered off, washed with methanol, and dried under vacuum at 50°C for 24 h.

Preparation of MWCNTs/PBZ nanocomposites

PBZ nanocomposites containing dispersed MWCNTs were prepared by the following procedures. The MWCNTs of 0.5, 1.0, 1.5, and 2.0 phr (part per hundred parts of resin) were first dispersed in tetrahydrofuran (THF), under ultrasonic vibration for 2 h. The MWCNTs/THF solutions with different MWCNTs weight fractions were then mixed with the B-m monomer. The solvent was then evaporated in a vacuum oven at 50°C for 1 day. The blended mixture was poured into a stainless-steel mold and polymerized in a stepwise manner, with heating at 120, 140, 160, and 200°C, each for 2 h. The product was postcured at 220 and 240°C for 30 min each.

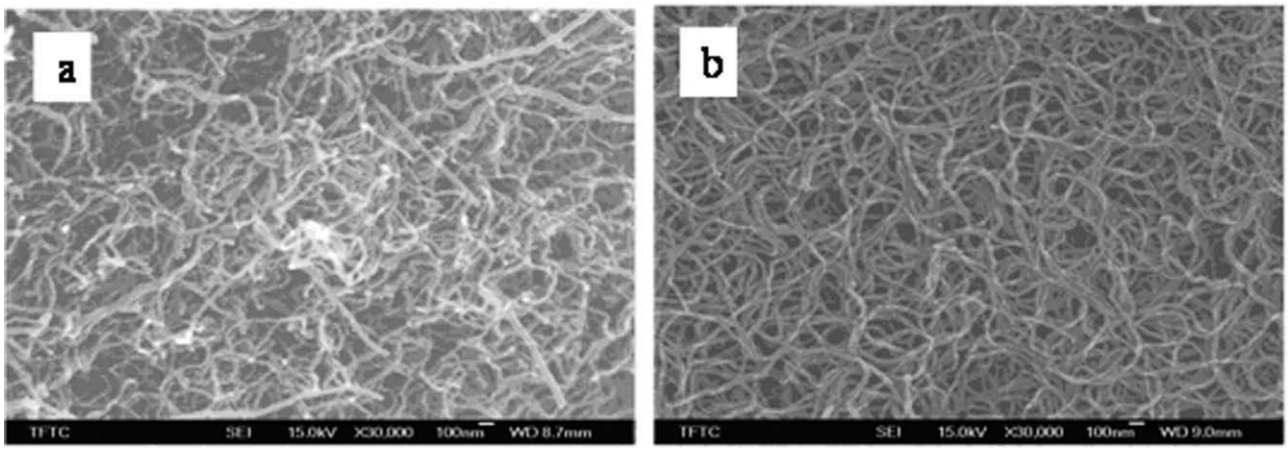

Figure 1 SEM micrographs of (a) the pristine and (b) microwave-purified (300 W, 5 min) MWCNTs.

Characterization

Fourier transform infrared spectroscopy

Infrared spectroscopy measurements were records on a Perkin–Elmer Spectra One Fourier transform infrared spectroscopy (FTIR) spectrometer with a spectral resolution of 1 cm^{-1}. FTIR was used to characterize the surface functionalities of the modified MWCNTs and to monitor the curing of the B-m monomer in the presence of MWCNT. Each sample was analyzed in the form of a potassium bromide (KBr) disc.

Differential scanning calorimetry

The calorimetric measurements were performed using a Perkin–Elmer DSC-7 differential scanning calorimeter operated under a N_2 atmosphere. The samples ($\sim$ 5 mg) were placed in a differential scanning calorimetry (DSC) pan and heated from 30 to 270°C at a heating rate of 10°C/min. The midpoint of the change in slope of the plot of the heat capacity during the heating scan was taken to be the glass transition temperature.

Dynamic mechanical analysis

DMA measurements were obtained using a TA Instruments DMA Q800 (TA Co., New Castle, DE, USA) instrument operated in a single-cantilever bending mode over the temperature range from 30 to 250°C. Data acquisition and analysis of the storage modulus (G'), loss modulus (G''), and loss tangent (tan δ) were recorded automatically by the system. The heating rate and frequency were fixed at 2°C/min and 1 Hz, respectively. Samples for DMA experiments were prepared by molding. The sample dimensions were 3 $\times$ 0.8 $\times$ 0.2 cm.

Thermomechanical analysis

Thermomechanical analysis (TMA) measurements were performed using a TA Instruments TMA Q400 (TA Co., New Castle, DE, USA). The force applied was 0.005*N*; the sample was heated from 30 to 250°C at a heating rate of 3°C/min.

Scanning electron microscopy

The morphologies of the MWCNTs were investigated using a Hitachi *S*-4700I (Japan) SEM operated at an accelerating potential of 10.0 kV.

Transmission electron microscopy

The morphologies of the MWCNTs/PBZ nanocomposites were investigated using an *S*-7100 TEM (Hitachi, Japan). A nanocomposite layer having a thickness of 100 nm was microtomed and then deposited onto a 200-mesh copper net for TEM observation.

Raman spectroscopy

The bonding structures of the pristine and modified CNTs were obtained using a Renishaw 2000 Raman spectrometer (He–Ne laser; 1 mW; 633 nm) equipped with a charge-coupled device (CCD) detector.

RESULTS AND DISCUSSION

SEM and TEM analysis of MWCNTs

Figure 1 presents SEM micrographs of the pristine and microwave-purified MWCNTs. The morphology of the pristine MWCNTs was enlaced congeries, presumably because strong Van der Waals forces between the surfaces of the CNTs made them susceptible to entanglement. The purified MWCNTs were more dispersed than that of the pristine MWCNTs, suggesting that irradiation with the

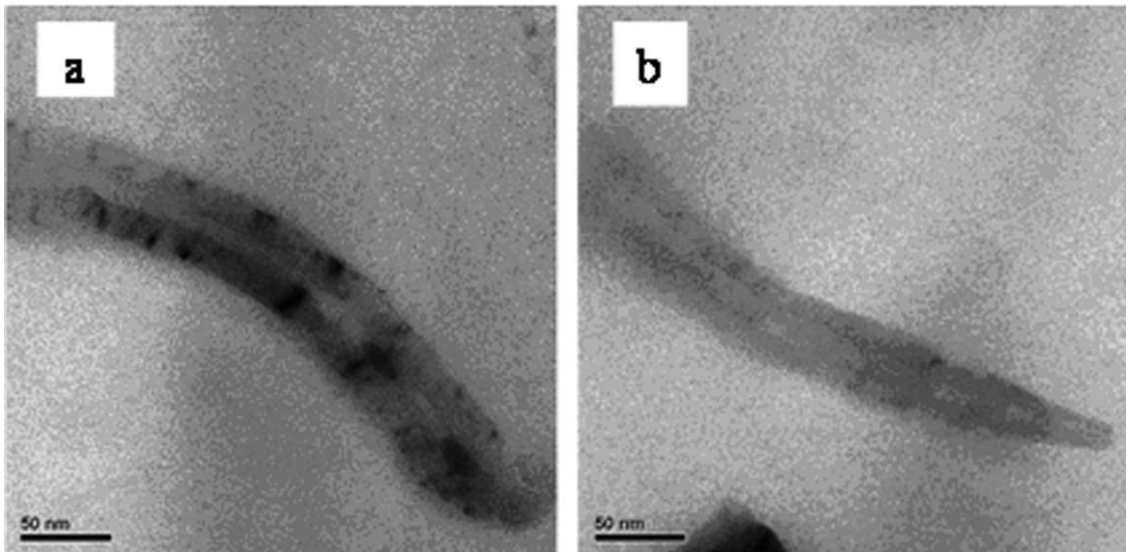

Figure 2 TEM images of (a) the pristine and (b) microwave-purified (300 W, 120°C, 40 min) MWCNTs.

microwaves had weakened the attraction between the MWCNTs' walls, causing them not to aggregate. It has been reported that microwave digestion can remove impurities from MWCNTs, thus improving their dispersion.[16] Figure 2 displays TEM images of the pristine MWCNTs and that had been purified under microwave irradiation at 300 W for 40 min. The pristine MWCNTs feature several impurities, such as amorphous carbon, graphite, and metals; after microwave digestion, the levels of these impurities had decreased dramatically. Most of the metal particles had dissolved because HNO_3 is a strong oxidant. The processing time required for microwave digestion to dissolve the metals in these MWCNTs was less than 1 h. Most acid-based purification methods for the removal of metal catalysts require more than 24 h; because HNO_3 treatment for such a long time will cleave MWCNTs into small pieces,[17,18] lower concentrations of acids, and shorter acid immersion times can be used to retain the wall structures of the MWCNTs. Using microwave purification allows metal catalysts to be dissolved in strong acids within short treatment times; therefore, it appears to be an effective, rapid method for the removal of metal particles from CNTs.

Raman spectroscopic analysis of MWCNTs

The Raman spectrum can discriminate between different types of graphite and carbon.[19,20] Figure 3 presents Raman spectra of the untreated MWNTs and the MWNTs subjected to microwave treatment. The peak near 1328 cm^{-1} is the D band, indicating disordered sp^2-hybridized carbon atoms. In contrast, the peak near 1583 cm^{-1} is the G band and is related to the graphitic E_{2g} symmetry of the interlayer mode. This mode reflects the structural integrity of the sp^2-hybridized carbon atoms of the nanotubes. The ratio of the intensities of the D and G bands is sensitive to the surface characteristics of the MWCNTs. For the pristine MWCNTs (Fig. 3a), the I_D/I_G ratio was 0.56. After microwave purification for 5, 10, 20, 30, and 40 min, the values decreased to 0.44, 0.42, 0.39, 0.34, and 0.29, respectively, indicating that the percentage of nanotube content improved after prolonged microwave treatment. Park et al.[21] also suggested that the I_G/I_D ratio would increase after purification because of the improvement in the nanotube percentage after eliminating amorphous carbon. On the contrary, when MWCNTs was treated with H_2SO_4 and HNO_3, the I_D/I_G ratio increased, indicating a decrease in order after acid modification; i.e., acid treatment produced

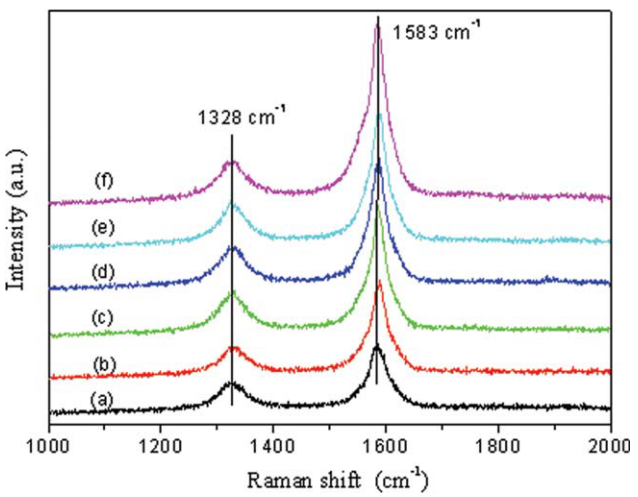

Figure 3 Raman spectra of (a) the pristine MWCNTs and (b–f) the MWCNTs purified at 300 W for (b) 5, (c) 10, (d) 20, (e) 30, and (f) 40 min. [Color figure can be viewed in the online issue, which is available at wileyonlinelibrary.com.]

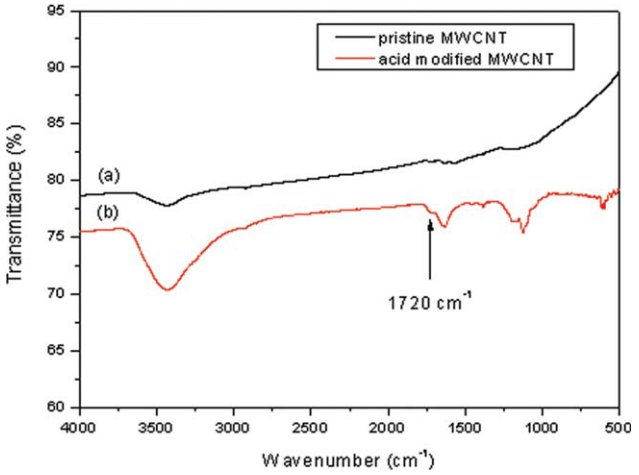

Figure 4 FTIR spectra of (a) the pristine and (b) modified MWCNTs. [Color figure can be viewed in the online issue, which is available at wileyonlinelibrary.com.]

carboxyl groups at local defects in the curved graphene and at the tube ends.

Characterization of modified MWCNTs

Figure 4 shows FTIR spectra of the pristine and modified MWCNTs. The spectrum of the pristine MWCNTs reveals peaks of very low intensity at 1650, 1173, and 3435 cm^{-1} corresponding to —C=O, —C—O, and —O—H stretching vibrations, respectively.[22] For the modified MWCNTs, these characteristic bands appeared with significantly higher intensities, consistent with their greater number of surface —COOH and —OH groups. In addition, the peak at 1720 cm^{-1} was clearly assigned to the —C=O stretching mode in the modified MWCNTs and indicated the successful formation of —COOH groups.[23]

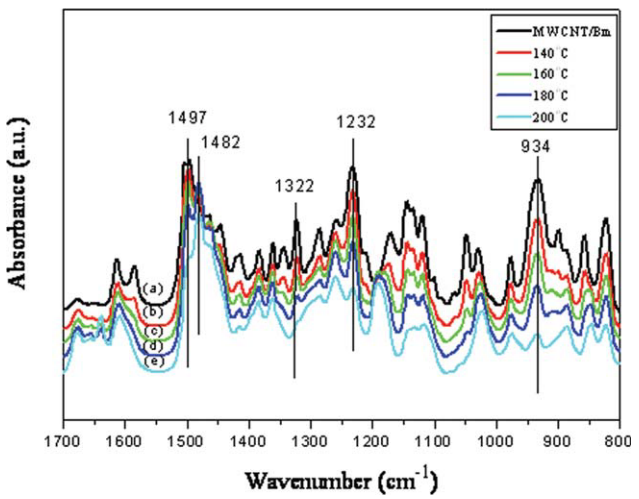

Figure 5 FTIR spectra of the 1 phr MWCNTs/B-m blend (a) before and (b–f) after curing for 1 h at (b) 140, (c) 160, (d) 180, and (e) 200°C. [Color figure can be viewed in the online issue, which is available at wileyonlinelibrary.com.]

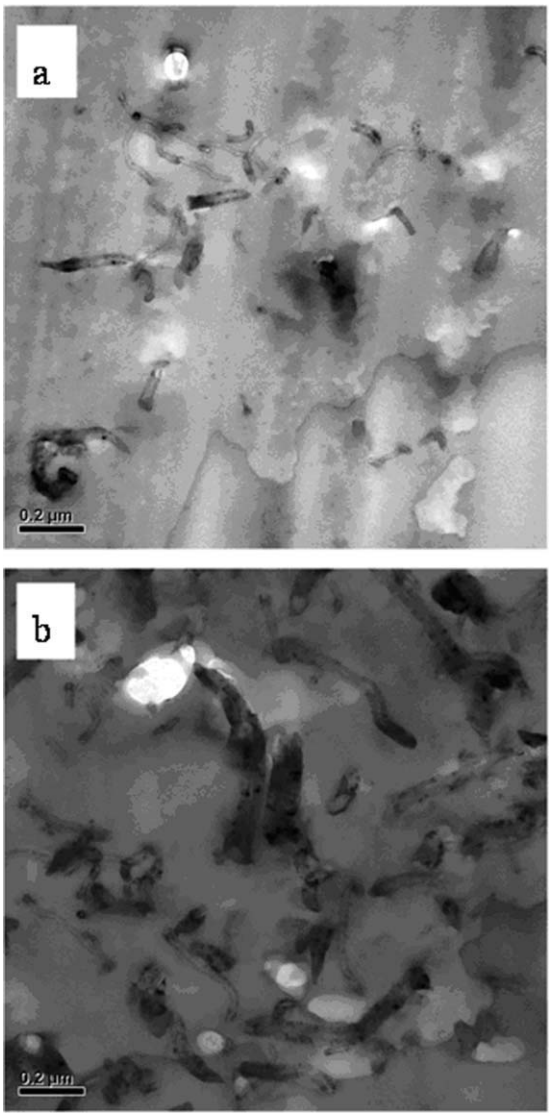

Figure 6 TEM images of MWCNTs/PBZ nanocomposites with (a) 1.0 and (b) 2.0 phr MWCNTs.

Curing reaction of MWCNTs/B-m blends

We used FTIR to investigate the curing behavior of the MWCNTs/B-m blends. Figure 5 displays FTIR spectra of the 1 phr MWCNTs/B-m blend at various curing stages. The characteristic absorptions of B-m at 934, 1232, 1322, and 1497 cm^{-1} gradually decreased, disappearing after curing at 200°C; one new peak appeared at 1482 cm^{-1}, attributable to the tetrasubstituted benzene ring,[1] that increased in intensity during the curing cycle. This signal is consistent with the ring opening of B-m to produce PBZ.

Morphology of MWCNTs/PBZ nanocomposites

Figure 6 shows the TEM images of MWCNTs/PBZ nanocomposites with 1.0 and 2.0 phr MWCNTs, respectively. From Figure 6a, we observe a random dispersion of the MWCNTs inside the PBZ matrix,

TABLE I
Glass Transition Temperatures (T_g) and Storage Moduli of PBZ and the MWCNTs/PBZ Nanocomposites

Composition	Storage modulus at 30°C (MPa)[a]	T_g (°C)	
		DSC	G″
PBZ	1004.6	183.0	185.1
0.5 phr MWCNTs/ PBZ = 0.005 g/1 g	1091.6	187.2	191.5
1.0 phr MWCNTs/ PBZ = 0.010 g/1 g	1124.2	190.1	193.2
1.5 phr MWCNTs/ PBZ = 0.015 g/1 g	1160.3	194.6	198.8
2.0 phr MWCNTs/ PBZ = 0.020 g/1 g	1137.4	192.5	196.0

[a] Standard deviation of the measurement was 2%.

without any serious agglomeration or clustering. The distribution of the MWCNTs in this sample was homogeneous. However, increasing the concentration of MWCNTs up to 2.0 phr resulted in their aggregation, as shown in Figure 6b. We attribute this behavior to the Van der Walls interactions among nanotubes as well as their high surface area and aspect ratio.

Glass transition temperature

We used DSC and DMA to measure the glass transition temperatures of the pure PBZ and MWCNTs/PBZ nanocomposites (Table I). The value of T_g determined through DSC increased from 183.0°C for the pure PBZ up to 190.1°C for the 1.0 phr MWCNTs/PBZ nanocomposites as shown in Figure 7. It appears that the well-dispersed MWCNTs limited the motion of the polymer chains, thus increasing the values of T_g of the nanocomposites. When the

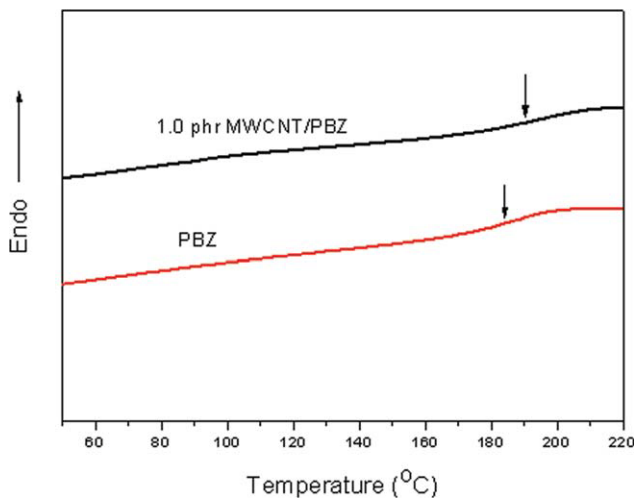

Figure 7 DSC thermograms of the pure PBZ and the 1.0 phr MWCNTs/PBZ blend. [Color figure can be viewed in the online issue, which is available at wileyonlinelibrary.com.]

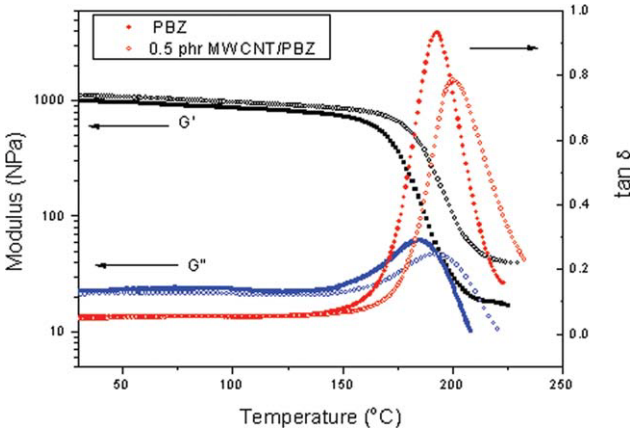

Figure 8 Storage moduli (G′), loss moduli (G″), and loss tangents (tan δ) of the pure PBZ and the 0.5 phr MWCNTs/PBZ nanocomposite. [Color figure can be viewed in the online issue, which is available at wileyonlinelibrary.com.]

MWCNTs content was greater than 1.5 phr, the adhesion between the MWCNTs and PBZ decreased and the T_g of the nanocomposites decreased as a result of aggregation of the MWCNTs.

Dynamic mechanical analysis

Figure 8 displays the temperature dependences of the storage moduli (*G′*), loss moduli (*G″*), and loss tangents (tan δ) of the pure PBZ and the 0.5 phr MWCNTs/PBZ nanocomposites, and the results are summarized in Table I. At 30°C, the storage moduli for the PBZ and the 0.5 phr MWCNTs/PBZ nanocomposite were 1004.6 and 1091.6 MPa, respectively. The storage modulus curves reveal an increase in the modulus intensity after incorporating the MWCNTs into the nanocomposite; the corresponding loss modulus curves reveal a decreased peak intensity accompanying an upward shift in temperature, which presumably arise primarily as a result of strong interactions between the components of the blend. We suspect that the MWCNTs bonded within the PBZ matrix hindered the motion of the molecular chains to some extent; thus, a higher temperature was required for activation. From the signal maximum in the *G″* curve, we determined the value of T_g of the pure PBZ to be ~ 185.1°C. For the 1.5 phr MWCNTs/PBZ nanocomposites, the corresponding value of T_g shifted to 198.8°C. Figure 9 shows the effect of MWCNTs content on the T_g of the nanocomposites. It is obvious that the T_g of the nanocomposites increases with the MWCNTs content up to 1.5 phr and then decreased for further increased to 2.0 phr. Thus, the viscoelastic properties revealed an increase in T_g for the PBZ matrix, arising from the nanometer-scale MWCNTs restricting the motion of the macromolecular chains in the nanocomposites.

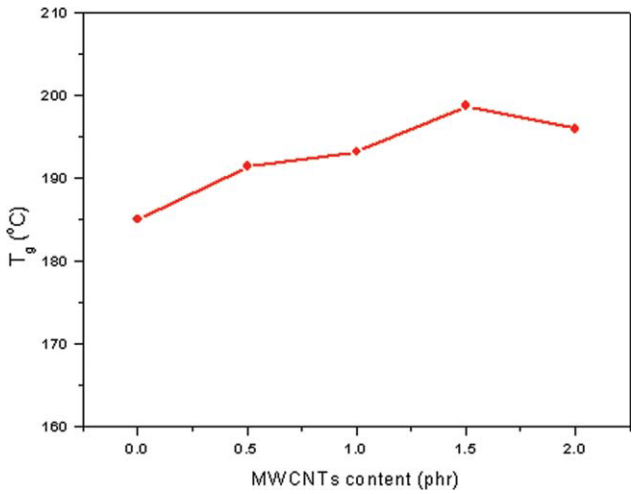

Figure 9 The effect of MWCNTs content on the T_g of the MWCNTs/PBZ nanocomposites. [Color figure can be viewed in the online issue, which is available at wileyonlinelibrary.com.]

In addition, the tan δ curves reveal a slight depression of the peak intensity after the incorporation of the MWCNTs. Because damping properties arise from the ratio of the viscous and elastics components, we surmise that the reduced peak height was associated with a lower segmental mobility and fewer relaxation species.

Coefficient of CTE

Dimensional stability is critical in many applications; poor dimensional stability can cause warping or other changes in shape. Pleasurably, these MWCNTs/PBZ nanocomposites exhibited improvements in both thermal and dimensional stabilities. The CTE of the pure PBZ was 66.2 μm/m°C; those of the MWCNTs/PBZ nanocomposites decreased on increasing the MWCNTs content, as shown in Figure 10. We attribute

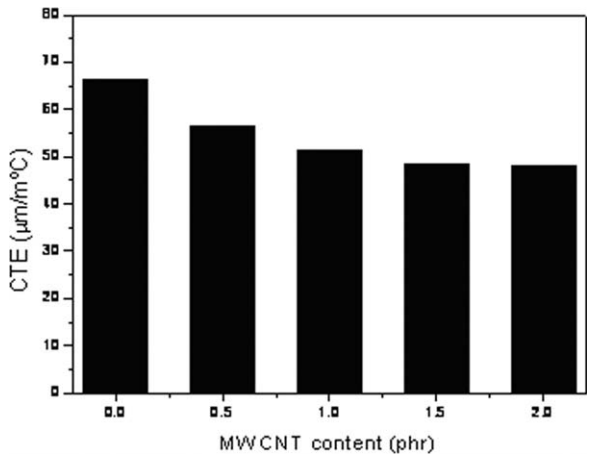

Figure 10 CTEs of the pure PBZ and the MWCNTs/PBZ nanocomposites with various MWCNTs contents.

these lower CTEs to the rigid and fine dispersion of the MWCNTs in the PBZ matrix. Thus, the incorporation of modified MWCNTs into PBZ can reduce the CTE and improve the thermal stability of the blends.

CONCLUSIONS

We prepared modified MWCNTs through microwave digestion followed by modification in a mixture of H_2SO_4 and HNO_3. FTIR spectrum revealed the presence of carboxyl and hydroxyl groups grafted onto the MWCNTs' surfaces. The carboxyl groups hydrogen bonded with the phenolic OH groups generated after the ring opening of benzoxazine, resulting in improved adhesion between PBZ and the MWCNTs. TEM micrographs confirmed that the MWCNTs were dispersed uniformly in the PBZ matrix when their content was less than 2 phr. DMA indicated increases in both the storage modulus and the value of T_g after the addition of the MWCNTs into the PBZ matrix; TMA revealed a corresponding decrease in the CTE.

We thank the National Science Council, Taiwan, Republic of China, for supporting this research financially under Contract No. 96-2221-E-238-001-MY3.

References

1. Ning, X.; Ishida, H. J Polym Sci A: Polym Chem Ed 1994, 32, 1121.
2. Ning, X.; Ishida, H. J Polym Sci B: Polym Phys Ed 1994, 32, 921.
3. Ishida, H.; Low, H. Y. Macromolecules 1997, 30, 1099.
4. Agag, T.; Takeichi, T. Macromolecules 2003, 36, 6010.
5. Lee, S. M.; Lee, Y. H. Appl Phys Lett 2000, 76, 2877.
6. Collins, P. G.; Bradley, K.; Ishigami, M.; Zettl, A. Science 2000, 287, 1801.
7. Deheer, W. A.; Chatelain, A.; Ugarte, D. Science 1995, 270, 1179.
8. Raravikar, N. R.; Schadler, L. S.; Vijayaraghavan, A.; Zhao, Y. P.; Wei, B. Q.; Ajayan, P. M. Chem Mater 2005, 17, 974.
9. Kim, Y. J.; Shin, T. S.; Choi, H. D.; Kwon, J. H.; Chung, Y. C.; Yoon, H. G. Carbon 2005, 43, 23.
10. Wang, R.; Sun, J.; Gao, L. J Phys Chem C 2010, 114, 4923.
11. Yang, L.; Zhang, C.; Pilla, S.; Gong, S. Composites A 2008, 39, 1653.
12. Chen, Q.; Xu, R.; Yu, D. Polymer 2006, 47, 7711.
13. Cui, S.; Canet, R.; Derre, A.; Couzi, M.; Delhaes, P. Carbon 2003, 41, 797.
14. Jang, J.; Yang, H. J Mater Sci 2000, 35, 2297.
15. Huang, J. M.; Yang, S. J Polymer 2005, 46, 8068.
16. Ko, F. H.; Lee, C. Y.; Ko, C. J.; Chu, T. C. Carbon 2005, 43, 727.
17. Moon, J. M.; An, K. H.; Lee, Y. H.; Park, Y. S.; Bae, D. J.; Park, G. S. J Phys Chem B 2001, 105, 5677.
18. Chiu, W. M.; Chang, Y. A. J Appl Polym Sci 2008, 107, 1655.
19. Tuinstra, F.; Koenig, J. L. J Chem Phys 1970, 53, 1126.
20. Tuinstra, F.; Koenig, J. L. J Compos Mater 1970, 4, 492.
21. Park, Y. S.; Choi, Y. C.; Kim, K. S.; Chung, D. C.; Bae, D. J.; An, K. H. Carbon 2001, 39, 655.
22. Tong, H.; Li, H. L.; Zhang, X. G. Carbon 2007, 45, 2424.
23. Wang, Y. B.; Iqbal, Z.; Mitra, S. Carbon 2005, 43, 1015.